Transport in Porous Media **6**: 115–142, 1991.
© 1991 *Kluwer Academic Publishers. Printed in the Netherlands.*

Displacement of a Newtonian Fluid by a Non-Newtonian Fluid in a Porous Medium

Y.-S. WU, K. PRUESS, and P. A. WITHERSPOON
Earth Sciences Division, Lawrence Berkeley Laboratory, Berkeley, CA 94720, U.S.A.

(Received: 7 July 1989; in final form: 3 June 1990)

Abstract. This paper presents an analytical Buckley–Leverett-type solution for one-dimensional immiscible displacement of a Newtonian fluid by a non-Newtonian fluid in porous media. The non-Newtonian fluid viscosity is assumed to be a function of the flow potential gradient and the non-Newtonian phase saturation. To apply this method to field problems a practical procedure has been developed which is based on the analytical solution and is similar to the graphic technique of Welge. Our solution can be regarded as an extension of the Buckley–Leverett method to Non-Newtonian fluids. The analytical result reveals how the saturation profile and the displacement efficiency are controlled not only by the relative permeabilities, as in the Buckley–Leverett solution, but also by the inherent complexities of the non-Newtonian fluid. Two examples of the application of the solution are given. One application is the verification of a numerical model, which has been developed for simulation of flow of immiscible non-Newtonian and Newtonian fluids in porous media. Excellent agreement between the numerical and analytical results has been obtained using a power-law non-Newtonian fluid. Another application is to examine the effects of non-Newtonian behavior on immiscible displacement of a Newtonian fluid by a power-law non-Newtonian fluid.

Key words. Non-Newtonian fluids, Buckley–Leverett, immiscible displacement, power-law fluids, rheological models, Welge method, fractional flow theory, enhanced oil recovery.

1. Nomenclature

Roman Letters

A	cross-sectional area (m^2)
f_{ne}	fractional flow of Newtonian phase
f_{nn}	fractional flow of non-Newtonian phase
$\mathbf{g}$	gravitational acceleration vector (m/s^2)
g	magnitude of the gravitational acceleration (m/s^2)
H	power law coefficient (Pa s^n)
K	absolute permeability (m^2)
k_{rne}	relative permeability of non-Newtonian phase
n	power-law exponential index
N_p	cumulative displaced Newtonian fluid (m^3)
P	pressure (Pa)
P_c	capillary pressure (Pa)
P_{ne}	pressure of Newtonian phase (Pa)
P_{nn}	pressure of non-Newtonian phase (Pa)

$q(t)$ injection rate of non-Newtonian fluid (m^3/s)
$Q(t)$ cumulative injection rate (m^3)
S_f saturation at moving front (m)
S_{ne} Newtonian phase saturation
S_{neir} irreducible Newtonian phase saturation
S_{nn} non-Newtonian saturation
S_{nnir} connate non-Newtonian saturation
$\bar{S}_{nn}$ average saturation of non-Newtonian phase in swept zone
x distance from inlet, coordinate (m)
x_f distance to shock saturation front (m)
$x_{s_{nn}}$ distance of saturation S_{nn} from the inlet (m)
t time (s)
u Darcy velocity (m/s)
$u(t)$ total flux (m/s)
u_{ne} Darcy velocity of Newtonian phase (m/s)
u_{nn} Darcy velocity of non-Newtonian phase (m/s)

Greek Letters

α angle between horizontal plane and flow direction
γ shear rate (s^{-1})
μ_{app} apparent viscosity (Pa s)
μ_{eff} effective viscosity (Pa s^n m^{1-n})
μ_{ne} viscosity of Newtonian fluid (Pa s)
μ_{nn} equivalent viscosity of non-Newtonian fluid (Pa s)
ρ_{ne} density of Newtonian fluid (kg/m^3)
ρ_{nn} density of non-Newtonian fluid (kg/m^3)
τ shear stress (Pa)
ϕ porosity of porous media
Φ flow potential (Pa)

Subscripts

app apparent
eff effective
f front
ne Newtonian
nn non-Newtonian
rne relative to Newtonian phase
rnn relative to non-Newtonian phase

2. Introduction

Immiscible flow of multiple phase fluids through porous media occurs in many subsurface systems. The behavior of multiple-phase flow, as compared with single-phase flow, is much more complicated and is not well understood in many areas due

to the complex interactions of different fluid phases. A fundamental understanding of immiscible displacement of Newtonian fluids in porous media was contributed by Buckley and Leverett (1942) in their classical study of the fractional flow theory. The Buckley–Leverett solution gave a saturation profile with a sharp front by ignoring the capillary pressure and gravity effects. A frequently encountered property of the Buckley–Leverett method is that the saturation becomes a multiple-valued function of the distance coordinate, x. This difficulty can be overcome by considering a material balance. Following the work of Buckley and Leverett (1942), a simple graphic approach was invented by Welge (1952), which can easily determine the sharp saturation front without the difficulty of the multiple-valued saturation problem for a uniform initial saturation distribution. More recently, some special analytical solutions for immiscible displacement, including the effects of capillary pressure, were obtained by Yortsos and Fokas (1983) and Chen (1983).

The Buckley–Leverett fractional flow theory has been applied and generalized by various authors to study the enhanced oil recovery (EOR) problems (Pope, 1980), surfactant flooding (Larson and Hirasaki, 1978) polymer flooding (Patton *et al.*, 1971), mechanism of chemical methods (Larson *et al.*, 1982), detergent flooding (Fayers and Perrine, 1959), displacement of oil and water by alcohol (Wachmann, 1964; Taber *et al.*, 1961), displacement of viscous oil by hot water and chemical additive (Karakas *et al.*, 1986), and alkaline flooding (DeZabala, *et al.*, 1982). An extension to more than two immiscible phases dubbed 'coherence theory' was described by Helfferich (1981). However, no non-Newtonian behavior has been considered in any of these works.

Non-Newtonian and Newtonian fluid immiscible displacement occurs in many EOR processes involving the injection of non-Newtonian fluids, such as polymer solutions, microemulsions, macroemulsions, and foam solutions. Almost all the theoretical and experimental studies performed on non-Newtonian fluid flow in porous media have focused on single non-Newtonian phase flow. Savins (1969) presented a comprehensive review of the flow of a non-Newtonian fluid through porous media. Scheidegger (1974) and Bird *et al.* (1960) summarized many rheological models for different non-Newtonian fluids. A very important contribution to study non-Newtonian flow in porous media was made by Gogarty (1967), who showed experimentally that the effective viscosity of pseudo-plastic fluid flow in a core depends upon the average shear rate, which is a function of pore velocity only, for a given porous material. The first analytical solutions, for a power-law non-Newtonian fluid were given simultaneously by Ikoku and Ramey (1979), and Odeh and Yang (1979) by using a linearization assumption. Their solutions have been extended by many authors to more complicated problems (Gencer and Ikoku, 1984; Ikoku, 1982, Ikoku and Ramey, 1980; Lund and Ikoku, 1981; and Vongvuthipornchai and Raghavan, 1987). A numerical method was also used to model non-Newtonian flow problems (Van Poolen and Jargon, 1969; McDonald, 1979).

Very little research has been published on multiple-phase flow of non-Newtonian and Newtonian fluids through porous media. To the best of our knowledge, there

is no analytical solution available. Even using numerical methods, very few studies have been conducted (Gencer and Ikoku, 1984). Therefore, the mechanism of immiscible displacement involving non-Newtonian fluids in porous media is still not well understood.

In this paper, an analytical solution describing the displacement mechanism of non-Newtonian/Newtonian fluid flow in porous media has been developed for one-dimensional linear flow. Our approach follows the classical work of Buckley and Leverett (1942) for the immiscible displacement of Newtonian fluids. The only important difference due to non-Newtonian behavior is in the fractional flow curve, which because of the velocity-dependent effective viscosity of a non-Newtonian fluid, now becomes dependent on the injection rate. A practical procedure for evaluating the behavior of non-Newtonian and Newtonian displacement is provided, based on the analytical solution, which is similar to the graphic method by Welge (1952). The resulting procedure can be regarded as an extension of the Buckley–Leverett theory to the flow problem of non-Newtonian fluids in porous media. The analytical results reveal how the saturation profile and the displacement efficiency are controlled not only by the relative permeabilities, as in the Buckley–Leverett solution, but also by the inherent complexities of non-Newtonian fluids.

The analytical solution developed here will find application in two areas: (1) it can be employed to study the displacement mechanisms of non-Newtonian and Newtonian fluid in porous media, and (2) it may be used to check numerical solutions from a simulator of non-Newtonian flow.

In addition, a numerical method has been used to simulate non-Newtonian and Newtonian multiple phase flow using the integral finite difference approach (Pruess and Wu; 1988). The numerical model can take into account all the important factors which affect the flow behavior of non-Newtonian and Newtonian fluids, such as capillary pressure, complicated flow geometry and operation conditions. The different rheological models for non-Newtonian fluid flow in porous media can easily be incorporated in the code. The validity of the numerical method has been checked by comparing the numerical results with those of the analytical solution, and excellent agreement has been obtained using a power-law, non-Newtonian fluid.

3. Mathematical Formulation

The two-phase flow of non-Newtonian and Newtonian fluids is considered in a homogeneous and isotropic porous medium. There is no mass transfer between the non-Newtonian and Newtonian phases, and dispersion and adsorption on rock are ignored. Then, the governing equations are given by

$$-\nabla \cdot (\rho_{ne} \mathbf{u}_{ne}) = \frac{\partial}{\partial t}(\rho_{ne} \; S_{ne} \phi) \tag{1}$$

for the Newtonian fluid, and

$$-\nabla \cdot (\rho_{nn} \mathbf{u}_{nn}) = \frac{\partial}{\partial t}(\rho_{nn} S_{nn} \phi) \tag{2}$$

for the non-Newtonian fluid. The Darcy velocities for the Newtonian and the non-Newtonian phase are described by a multiphase extension of Darcy's law as

$$\mathbf{u}_{ne} = -K \frac{k_{rne}}{\mu_{ne}} (\nabla P_{ne} - \rho_{ne} \mathbf{g}) \tag{3}$$

and

$$\mathbf{u}_{nn} = -K \frac{k_{rne}}{\mu_{nn}} (\nabla P_{nn} - \rho_{nn} \mathbf{g}). \tag{4}$$

The pressures in the two phases are related by means of the capillary pressure

$$P_c(S_{nn}) = P_{ne} - P_{nn}. \tag{5}$$

The relative permeabilities, k_{rne}, k_{rnn}, and the capillary pressure P_c are assumed to be functions of saturation only. Also, from the definition of saturation, we have

$$S_{ne} + S_{nn} = 1.$$

4. Analytical Solution

For the derivation of the analytical solution, the following additional assumptions are made

(1) the two fluids and the porous medium are incompressible,
(2) the capillary pressure gradient is negligible,
(3) the apparent viscosity of non-Newtonian fluids is a function of the flow potential and saturation,

$$\mu_{nn} = f(S_{nn}, \nabla \Phi,), \tag{7}$$

where $\nabla\Phi$ is the flow potential gradient, a vector. Its component in the x coordinate is

$$\frac{\partial \Phi}{\partial x} = \frac{\partial P}{\partial x} + \rho_{nn} g \sin \alpha. \tag{8}$$

By definition, the viscosity of a non-Newtonian fluid is a function of the shear rate. For flow through porous media, it has been shown that the shear rate depends only on the pore velocity for a given porous material (Gogarty, 1967). The pore velocity is determined by the local potential gradient and by the local saturation within the two-phase fluid. We assume that the viscosity of the non-Newtonian fluid is described by Equation (7) for multiple-phase flow, which should be determined by experiment for the non-Newtonian fluid and the porous medium of interest.

The flow system considered is a semi-infinite linear reservoir, shown in Figure 1. It is further assumed that gravity segregation is negligible and that stable displacement exists near the displacement front. Then, Equations (1) and (2) become

$$-\frac{\partial u_{ne}}{\partial x} = \phi \frac{\partial S_{ne}}{\partial t} \tag{9}$$

and

$$-\frac{\partial u_{nn}}{dx} = \phi \frac{\partial S_{nn}}{\partial t}. \tag{10}$$

For the Newtonian phase, the flow rate is

$$u_{ne} = -K \frac{k_{rne}}{\mu_{ne}} \left(\frac{\partial P}{\partial x} + \rho_{ne} g \sin \alpha \right) \tag{11}$$

and for the non-Newtonian phase,

$$u_{nn} = -K \frac{k_{rnn}}{\mu_{nn}} \left(\frac{\partial P}{\partial x} + \rho_{nn} g \sin \alpha \right). \tag{12}$$

To complete the mathematical description, the initial and boundary conditions must be specified. Initially, a Newtonian fluid is at its maximum saturation in the system.
Thus,

$$S_{ne}(x, 0) = 1 - S_{nnir}, \tag{13}$$

where S_{nnir} is the initial immobile non-Newtonian fluid saturation. For practical field problems, S_{nnir} is usually zero, which can be treated as a special case. In this problem, we are concerned with continuously injecting a non-Newtonian fluid from the inlet $x = 0$, at a known rate $q(t)$, which can be a function of injection time, t.

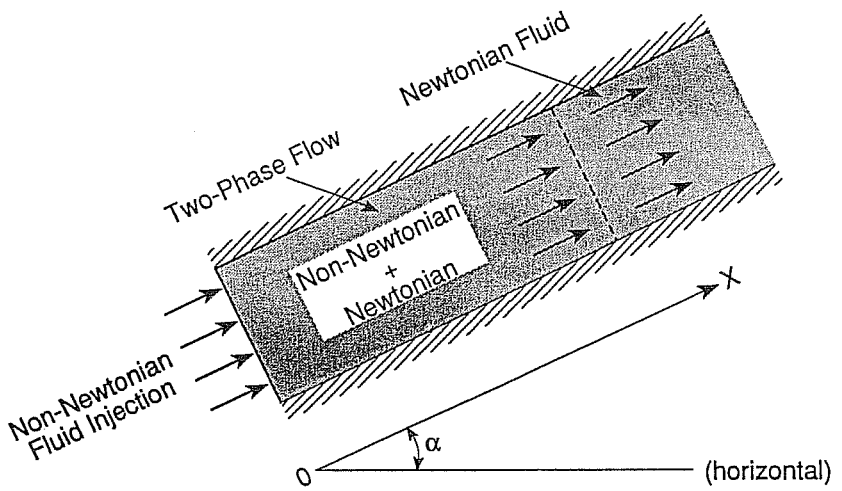

Fig. 1. Schematic of displacement of a Newtonian fluid by a non-Newtonian fluid.

The boundary conditions at $x = 0$ are

$$u_{nn}(0, t) = u(t) = \frac{q(t)}{A}, \tag{14}$$

$$u_{ne}(0, t) = 0, \tag{15}$$

where A is the cross-sectional area for flow. Finally, in a semi-infinite system, the following conditions must be imposed at $x \to \infty$,

$$S_{ne} \to 1 - S_{nnir} \tag{16}$$

and

$$S_{nn} \to S_{nnir}. \tag{17}$$

The governing equations (9), (10) with the boundary and initial conditions (13)–(17), can be solved to obtain the following solution (see Appendix A):

$$\left(\frac{dx}{dt}\right)_{S_{nn}} = \frac{q(t)}{\phi A}\left(\frac{\partial f_{nn}}{\partial S_{nn}}\right)_t. \tag{18}$$

This is the frontal advance equation for the non-Newtonian displacement, and is the same in form as the Buckley–Leverett equation. The difference is the dependence of the fractional flow f_{nn} for the non-Newtonian displacement on saturation not only through the relative permeability, but also through the non-Newtonian phase viscosity, which is a function of both potential gradient and saturation. For a given time, a given injection rate, and given fluid and rock properties, the potential gradient can be shown using Equation (A6) to be a function of saturation only. Equation (18) shows that a particular non-Newtonian fluid saturation profile propagates through the porous medium at a constant velocity for a given time and injection rate. As in the Buckley–Leverett theory, the saturation for a vanishing capillary pressure gradient will, in general, become a triple-valued function of distance near the displacement front. Equation (18) will then fail to describe the velocity of the shock saturation front, since $\partial f_{nn}/\partial S_{nn}$ does not exist on the front. Consideration of material balance across the shock front (Sheldon *et al.*, 1959) provides the velocity of the front

$$\left(\frac{dx}{dt}\right)_{S_f} = \frac{q(t)}{A\phi}\left[\frac{f_{nn}^+ - f_{nn}^-}{S_{nn}^+ - S_{nn}^-}\right], \tag{19}$$

where S_f is the front saturation of the displacing non-Newtonian phase. The superscripts '+' and '−' refer to values ahead of and behind the shock, respectively.

The location $x_{S_{nn}}$ of any saturation S_{nn} traveling from the inlet can be determined by integrating Equation (18) with respect to time, which yields

$$x_{S_{nn}} = \frac{Q(t)}{A\phi}\left(\frac{\partial f_{nn}}{\partial S_{nn}}\right)_{S_{nn}}, \tag{20}$$

where $Q(t)$ is the cumulative volume of injected fluid

$$Q(t) = \int_0^t q(\lambda)\, d\lambda. \tag{21}$$

A direct use of Equation (20), given x and t, will result in a multiple-valued saturation distribution, which can be handled by a mass balance calculation, as in the Buckley–Leverett solution. An alternative graphical method of evaluating the above solution will be discussed in the next section.

5. Graphical Evaluation Method

The fractional flow of the displacing non-Newtonian phase is a function of its saturation only, after taking into account the constraint condition (A6). Therefore, the Welge (1952) graphic method can be shown to apply for evaluation of non-Newtonian fluid displacement by an integration of the mass balance of injection into the system and incorporation of Equation (20). The only additional constraint is the need to take into account the contribution of a velocity-dependent, effective viscosity of non-Newtonian fluids on the fractional flow curve. At the moving saturation front, we have (see Appendix B).

$$\left(\frac{\partial f_{nn}}{\partial S_{nn}}\right)_{S_f} = \frac{f_{nn}|_{S_f} - f_{nn}|_{S_{nnir}}}{S_f - S_{nnir}} \tag{22}$$

and the average saturation in the displaced zone is given by

$$\left(\frac{\partial f_{nn}}{\partial S_{nn}}\right)_{S_f} = \frac{1}{\bar{S}_{nn} - S_{nnir}}, \tag{23}$$

where $\bar{S}_{nn}$ is the average saturation of the non-Newtonian phase in the swept zone. To satisfy Equations (22) and (23), a simple geometric construction can be used (see Figure 2). On a curve of fractional flow f_{nn} versus saturation S_{nn}, draw the tangent to the fractional flow curve, from the point $(S_{nn} = S_{nnir}, f_{nn} = 0)$. The point of tangency has coordinates $(S_{nn} = S_f, f_{nn} = f_{nn}|_{S_f})$, and the extrapolated tangent must intercept the line $f_{nn} = 1$ at the point $(S = S_{nn}, f_{nn} = 1)$. Therefore, the graphic method of Welge applies if the fractional flow curves are provided for the non-Newtonian displacement process. The only difference is in the determination of the non-Newtonian fractional flow curve because we have to include the effects of the apparent viscosity of non-Newtonian fluids, which are also a function of saturation.

With given relative permeability data and the rheological model μ_{nn}, the general procedure for evaluating the flow behavior of non-Newtonian one-dimensional linear displacement is as follows:

(1) Solve pressure gradients $-\partial P/\partial x$, from Equation (A6) for different injection rate and plot the relationship between pressure gradient and saturation corresponding to the injection rate, as shown in Figure 3. This requires use

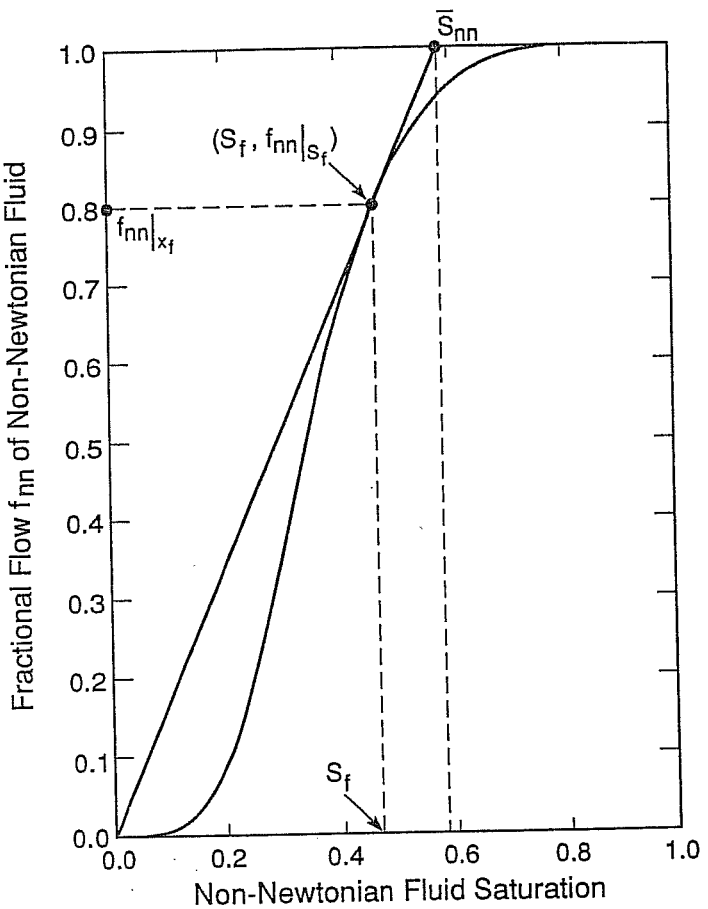

Fig. 2. Method of determining shock front and average displacing non-Newtonian phase saturations from fractional flow curves.

of the equivalent non-Newtonian viscosity as derived in Appendix C, Equation (C8).

(2) Calculate the fractional flow, f_{nn}, by Equation (A8), using the pressure gradients from Figure 3 to calculate the corresponding potential gradients, then, using Equation (C8), to compute the non-Newtonian phase viscosity. An example of fractional flow curves is shown in Figure 4.

(3) Calculate the derivatives of fractional flow, $\partial f_{nn}/\partial S_{nn}$, with respect to saturation from Figure 4. These are shown in Figure 5.

(4) Determine the shock front saturation from Figure 4, as illustrated in Figure 2.

(5) Calculate the saturation profile for $S_f < S_{nn} < 1 - S_{neir}$ from $x = 0$ to $x = x_f$ according to Equation (20) for a given injection rate and using the corresponding potential gradients from Figure 5. This profile is shown in Figure 6.

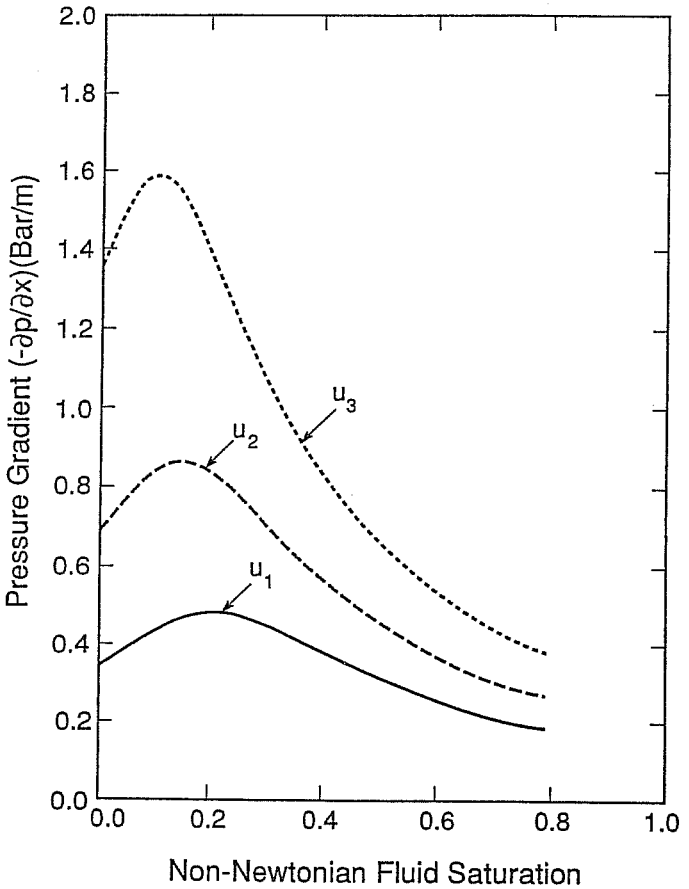

Fig. 3. Pressure gradients versus displacing non-Newtonian phase saturation for different injection rates.

(6) Determine the average saturation in the swept zone from Figure 4, as illustrated in Figure 2. This can be used to calculate the cumulative Newtonian fluid displaced, N_p,

$$N_p = A\phi x_f(\bar{S}_{nn} - S_{nnir}). \tag{24}$$

The above procedure has been programmed for use in this work.

6. Comparison with Numerical Simulation

A numerical simulator (MULKOM-GWF), which is a modified version of MULKOM (Pruess, 1983; Pruess and Wu, 1988), has been developed for modeling multiple-phase flow of non-Newtonian and Newtonian fluids in porous media under a wide range of operating conditions and with different rheological models

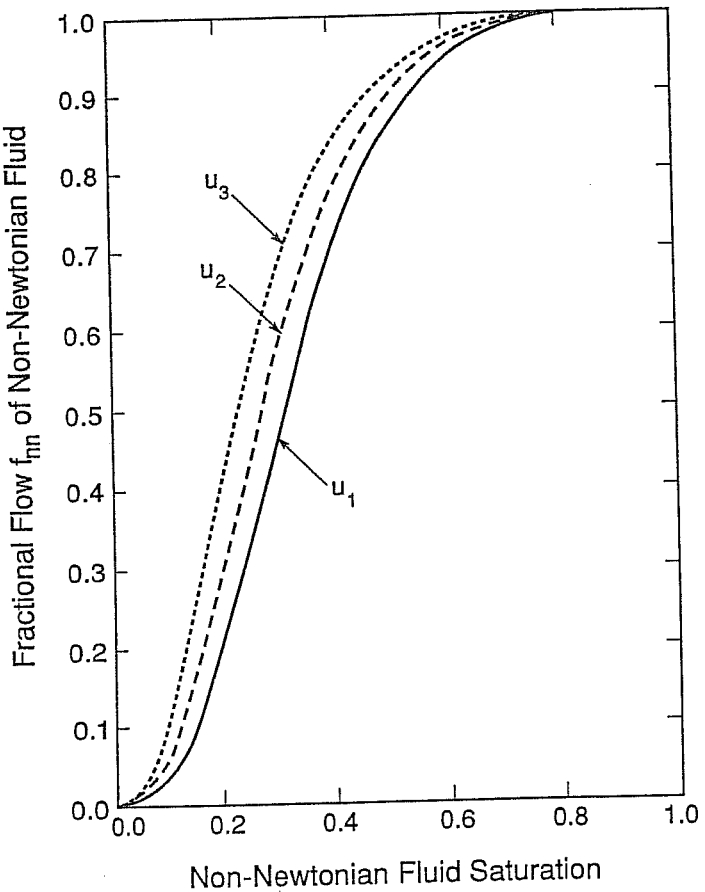

Fig. 4. Fractional flow curves of non-Newtonian fluids for different injection rates.

for the non-Newtonian fluid behavior. We have programmed an equivalent non-Newtonian viscosity given by Equation (C8) into the simulator. The validity of the numerical results from this code has been tested for immiscible displacement of a Newtonian fluid by a non-Newtonian fluid by comparison with the Buckley–Leverett type solution obtained above. The example of interest is a one-dimensional linear flow problem of incompressible two-phase fluids in a semi-infinite, horizontal homogeneous and isotropic porous medium. A constant injection rate is maintained at the inlet ($x = 0$) from time $t = 0$. Initially, the reservoir is fully saturated with only the Newtonian liquid. The relative permeability curve used for both the analytical and numerical calculations is shown in Figure 7. Capillary effects are assumed to be negligible.

In order to reduce the effects of discretization in a finite system, very fine mesh spacing ($\Delta x = 0.0125$ m) was chosen for the first 240 elements, then the mesh spacing was increased by a factor of 1.5 to the 290th element. The non-Newtonian

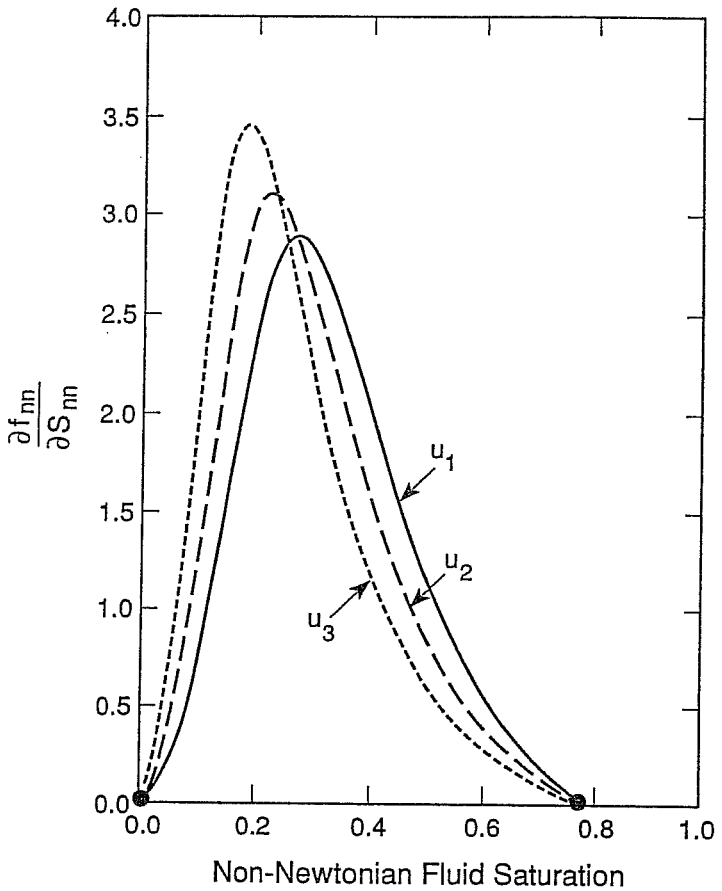

Fig. 5. Derivatives of fractional flow with respect to non-Newtonian phase saturation for different injection rates.

displacement analytical solution was evaluated by using the computer-graphic method outlined in the previous section. The power-law non-Newtonian fluid has been used extensively in the study of non-Newtonian fluid flow through porous media both theoretically and experimentally. To demonstrate the applicability of the analytical solution, a power-law liquid was used as a displacing agent to drive the initially saturated Newtonian liquid in the porous medium.

The properties of rock and fluids are given in Table I. If we assume a power-law index of $n = 0.5$, then the pressure gradients for horizontal flow can be derived from Equation (A6) as

$$-\frac{\partial P}{\partial x}=\frac{1}{2}\left\{\left[\frac{\left(\frac{Kk_{rne}}{\mu_{ne}}\right)^2}{\frac{Kk_{rnn}}{\mu_{eff}}}+\frac{4q}{\left(\frac{Kk_{rnn}}{\mu_{eff}}\right)^{1/2}}\right]^{1/2}-\frac{\frac{Kk_{rne}}{\mu_{ne}}}{\left(\frac{Kk_{rnn}}{\mu_{eff}}\right)^{1/2}}\right\}. \tag{25}$$

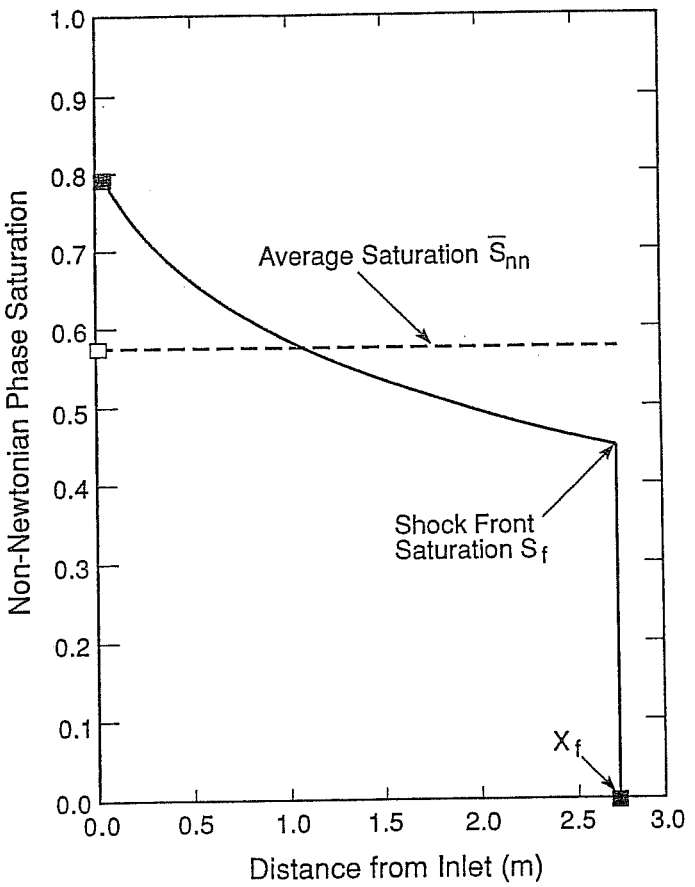

Fig. 6. Saturation distributions of non-Newtonian fluids in the system at a given injection time.

Table I. Parameters for linear power-law fluid displacement

Porosity	$\phi = 0.20$
Permeability	$K = 1$ darcy
Cross-sectional area	$1\ m^2$
Injection rate	$q = 0.8233 \times 10^{-5}\ m^3/s$
Injection time	$T = 10$ h
Displaced phase viscosity	$\mu_{ne} = 5$ cp
Irreducible Newtonian saturation	$S_{neir} = 0.20$
Initial non-Newtonian saturation	$S_{nnir} = 0.00$
Power-law index	$n = 0.5$
Power-law coefficient	$H = 0.001$ Pa s^n

Equation (25) was used in calculating the fractional flow f_{nn} to incorporate the non-Newtonian flow effects in the analytical solution. A comparison of the saturation profiles from the numerical and analytical calculations after 10 h of non-Newtonian fluid injection into the system is given in Figure 8. This shows that the numerical results are in excellent agreement with the analytical prediction. Consid-

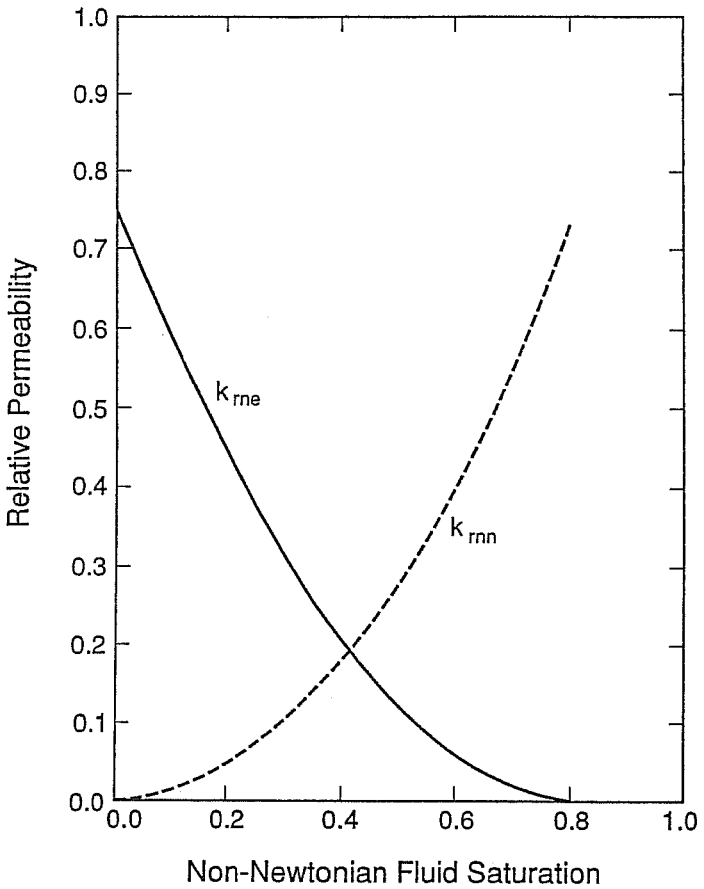

Fig. 7 Relative permeability functions used for all calculations.

ering the complexity introduced when non-Newtonian fluids are involved in a multiple phase flow problem, Figure 8 provides a very encouraging indication that the numerical model is correct in describing the multiple phase immiscible displacement of non-Newtonian and Newtonian fluid flow in porous media. The viscosity profiles of the non-Newtonian fluid are given in Figure 9, and show good agreement between the analytical and numerical results over the whole non-Newtonian fluid swept region, $x < x_f$. Only at the shock advancing saturation front does the numerical solution deviate somewhat from the analytical solution, which is a typical 'smearing front' effect from numerical dispersion there.

7. Discussion of Non-Newtonian Displacement

For a given operating condition, non-Newtonian fluid displacement in porous media is controlled not only by relative permeability effects, as in Newtonian fluid

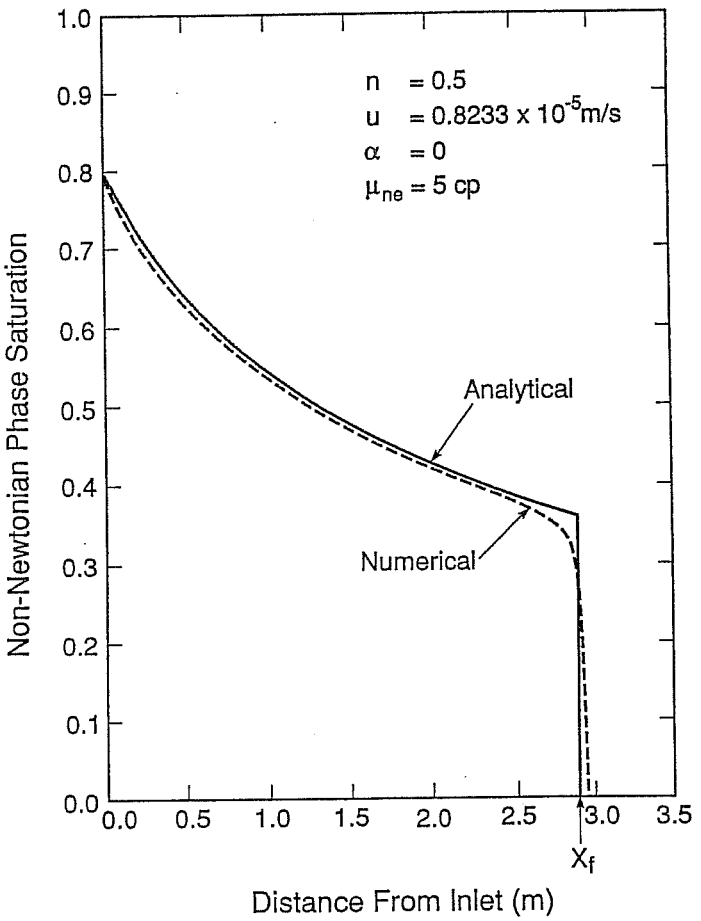

Fig. 8. Comparison of saturation profiles calculated from analytical and numerical solutions after 10 h of injection.

displacement, but also by the non-Newtonian fluid rheological properties. Some fundamental behavior of power-law non-Newtonian fluid displacement will be disussed in this section by using results from the analytical solution.

7.1. EFFECTS OF INJECTION RATE

For Newtonian displacement in porous media based on Buckley–Leverett solutions, the injection rate has no effect on displacement efficiency or sweep efficiency. When a non-Newtonian fluid is involved, changes in the injection rate will result in changes in the pore velocity, which will affect the viscosity of the non-Newtonian phase and fractional flow curve. The fluid and rock parameters used for the

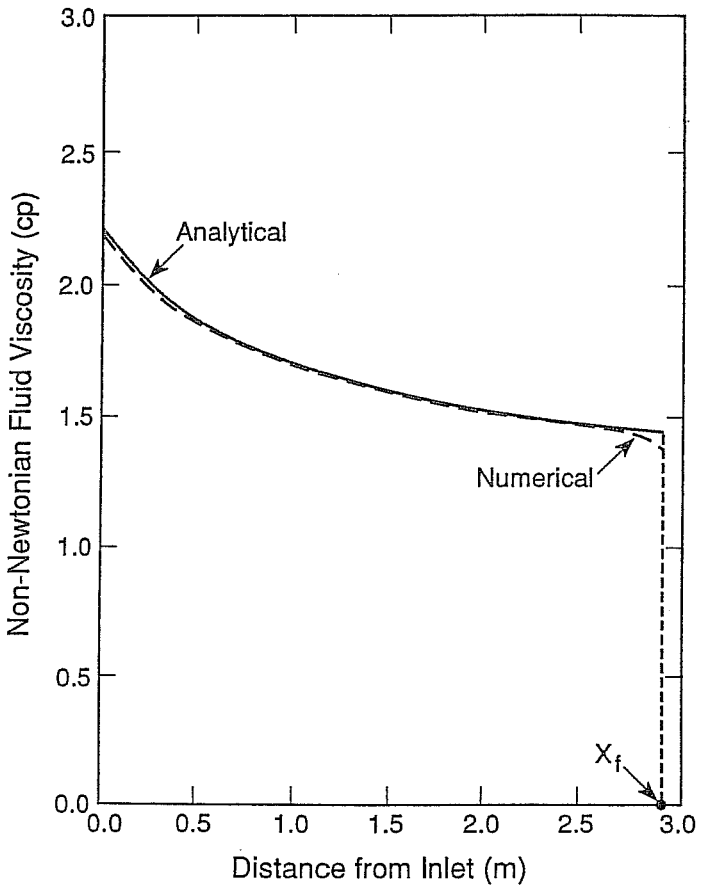

Fig. 9. Comparison of non-Newtonian fluid equivalent viscosity profiles calculated from analytical and numerical solutions after 10 h of injection.

calculations in this section are similar to those used in the previous section, and any differences are indicated on the figures to follow. Figure 10 gives non-Newtonian viscosity versus saturation curves for three different injection rates in a semi-infinite linear horizontal system. Considering the constraint condition (A6), the viscosity of non-Newtonian fluids depends only on the non-Newtonian phase saturation. The resulting saturation profiles corresponding to the injection rates are shown in Figure 11. The horizontal lines are the average saturations in the swept zone, which reflect the sweep efficiency. Since the only variable parameter in this calculation is the injection rate, the saturation distributions in Figure 11 indicate that injection rate has a significant effect on displacement. For a displacement process with this type of shear thinning fluid, the lower the injection rate, the higher the displacement efficiency becomes.

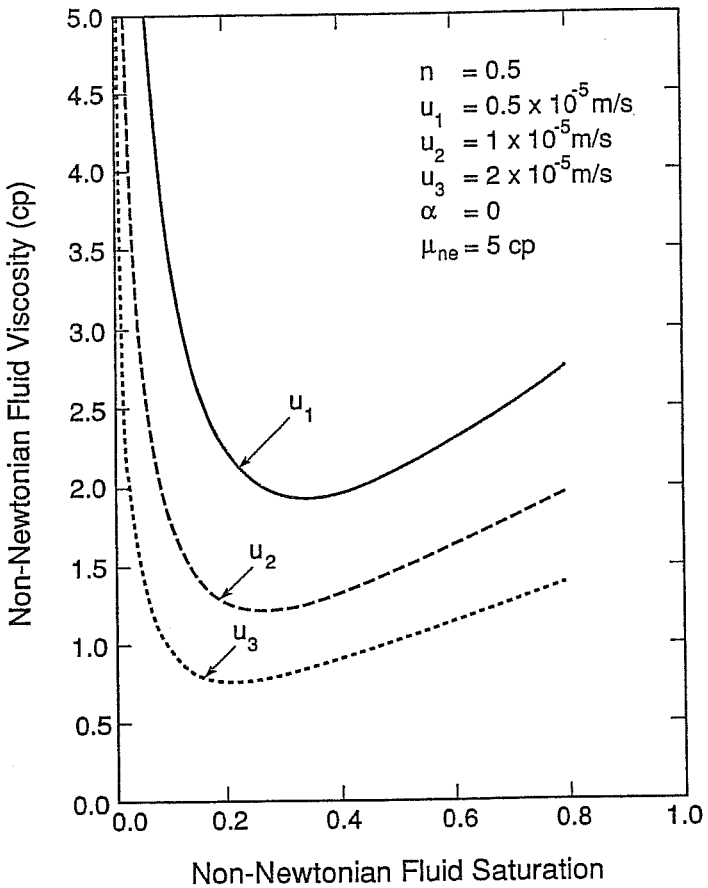

Fig. 10 Non-Newtonian phase apparent viscosities versus non-Newtonian phase saturation for different injection rates.

7.2. EFFECTS OF POWER-LAW INDEX-n

There are two parameters that characterize the flow behavior of a power-law fluid, the exponential index, n, and coefficient, H. For a pseudoplastic fluid, $0 < n < 1$. If $n = 1$, the fluid is Newtonian. The effect of the power-law index, n, on linear horizontal displacement can be quite significant. Figure 12 shows that pressure gradients are changed tremendously as a function of saturation for different values of n. The apparent viscosities of several non-Newtonian fluids are given in Figure 13, and the resulting fractional flow curves are shown in Figure 14. Saturation profiles after a 10 h injection period in the system are plotted in Figure 15. Note the significant differences in sweep efficiency.

Since the power-law index, n is usually determined from an experiment or from well test analysis, some errors cannot be avoided in determining the values of n.

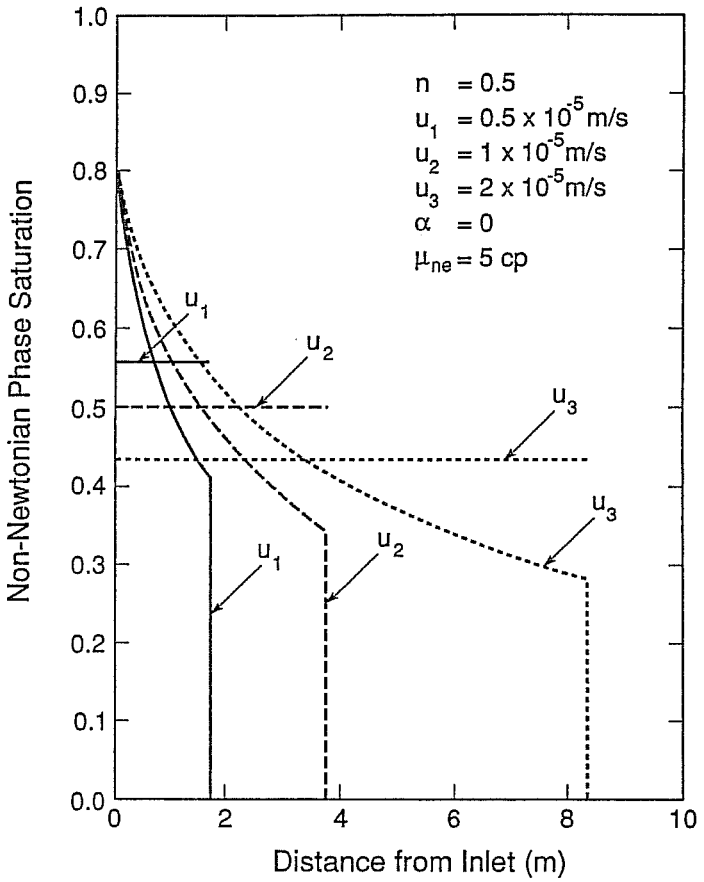

Fig. 11. Non-Newtonian phase saturation distributions for different injection rates after 10 h of injection.

These results show how difficult it will be to use a numerical code to match experimental data from non-Newtonian displacement investigations in the laboratory, because of the extreme sensitivity of the core saturation distribution to n. The sensitivity of the displacement behavior to the power-index n suggests that in determining the index n, it may be helpful to match experimental saturation profiles using the analytical solution.

7.3. EFFECTS OF GRAVITY

It is expected that gravity may have more significant effects on non-Newtonian displacement than on Newtonian displacement, because it influences mobility by affecting the non-Newtonian phase viscosity, in addition to the effect on the

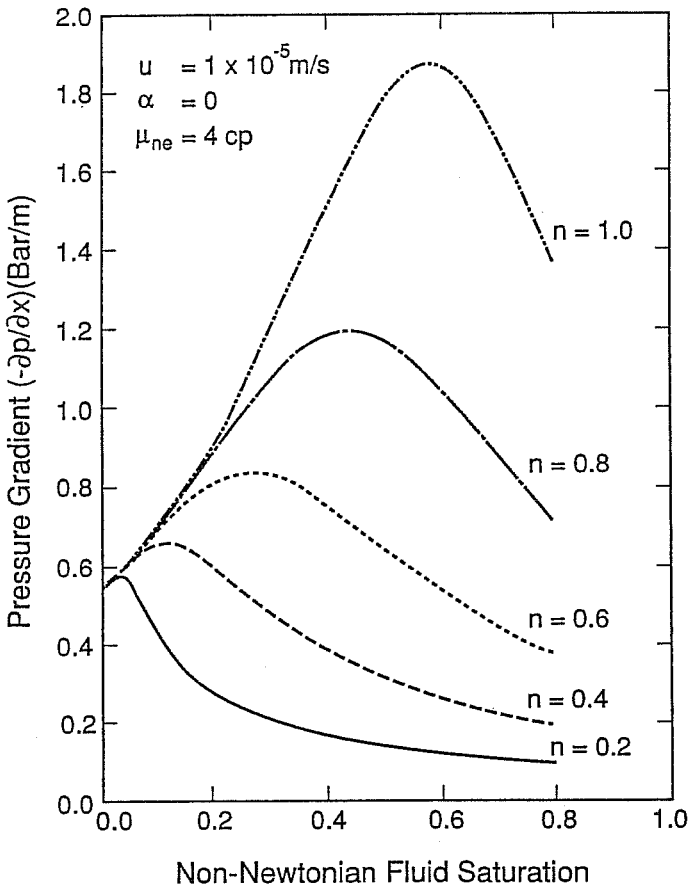

Fig. 12. Effects of the power-law index on pressure gradients.

potential gradient as in Newtonian displacement. This can be demonstrated by the following example. A power-law non-Newtonian fluid is injected upwards ($\alpha = \pi/2$), horizontally ($\alpha = 0$), and downwards ($\alpha = -\pi/2$), to displace a heavier *in-situ* Newtonian fluid. The fractional flow curves are given in Figure 16. Since counterflow may occur physically at very low or very high displacing phase saturations under gravity effects, we will have the situations that $f_{nn} > 1$ for upflow and $f_{nn} < 0$ for downflow. The final saturation distributions in Figure 17 show the significance of effects of gravity on non-Newtonian displacement in porous media.

8. Conclusions

An analytical solution for describing the displacement of a Newtonian fluid by a non-Newtonian fluid through porous media has been developed. A general viscosity function for non-Newtonian fluids is proposed and used in the solution, which

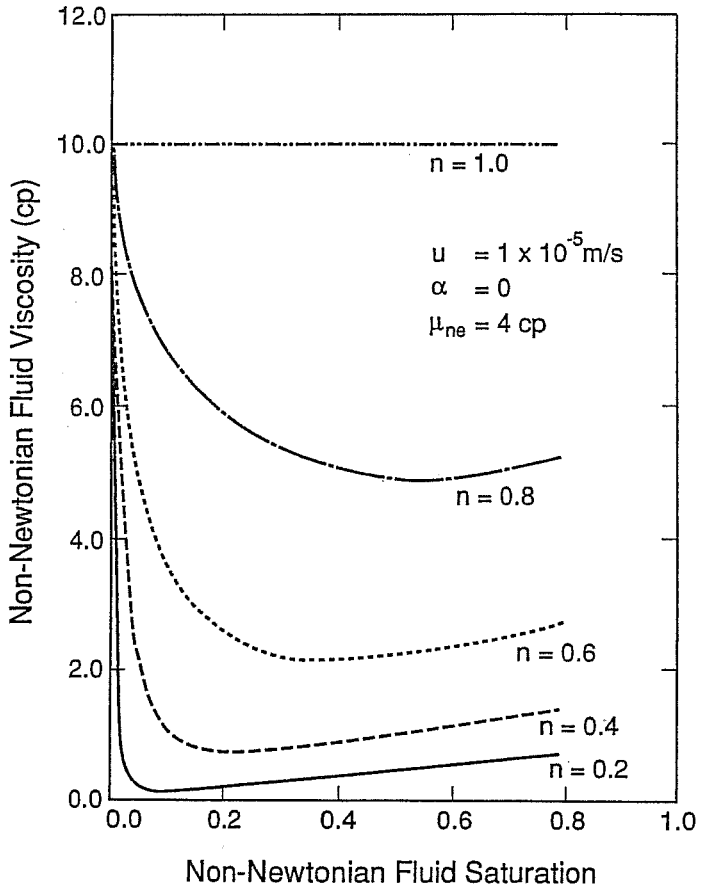

Fig. 13. Effects of the power-law index on non-Newtonian phase equivalent viscosity.

relates non-Newtonian phase viscosity to the local potential gradient and saturation, and is suitable for different rheological models of non-Newtonian fluids. The analytical solution is applicable to displacement of a non-Newtonian fluid by a Newtonian fluid or to displacement of a non-Newtonian fluid by another non-Newtonian fluid.

Two examples of application of the analytical solution are presented. First, it is used to verify a numerical simulator for multiple-phase flow involving a non-Newtonian fluid. Secondly, it is used to obtain insight into the physics of non-Newtonian displacement in porous media. The calculated analytical results reveal that non-Newtonian dispacement is a complicated process, controlled by the rheological properties of non-Newtonian fluids used, and the injection condition, in addition to relative permeability, and is more sensitive to gravity effects as well.

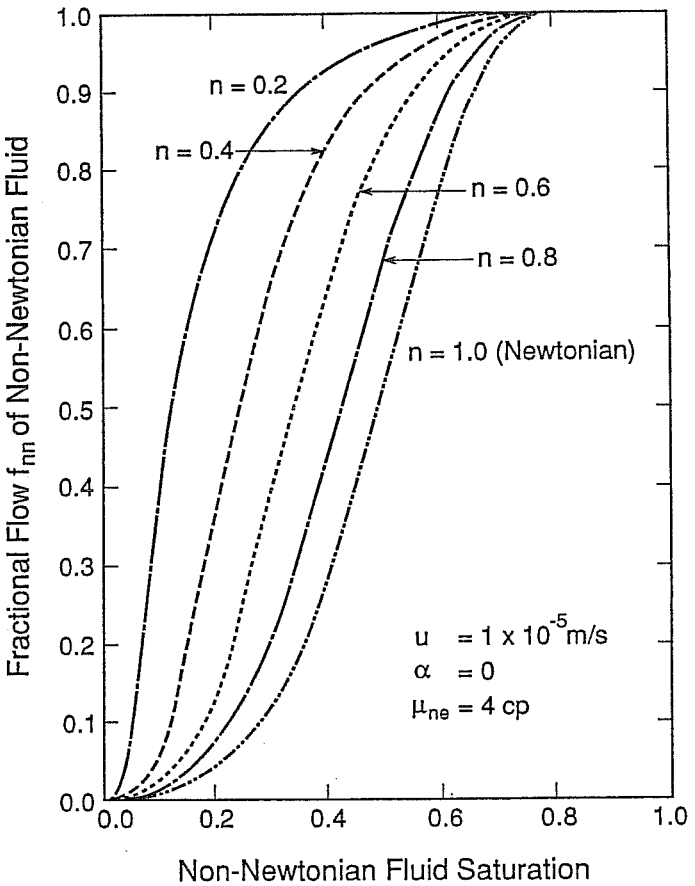

Fig. 14. Effects of the power-law index on non-Newtonian phase fractional flow.

Appendix A: Derivation of Buckley–Leverett-Type Solution

The sum of equations (9) and (10) gives

$$-\frac{\partial(u_{ne}+u_{nn})}{\partial x}=\phi\frac{\partial}{\partial t}(S_{ne}+S_{nn})=0. \tag{A1}$$

This means that at a given time, the total volumetric flow rate through any cross-section in the flow system is independent of the distance coordinate, x.

$$u_{ne}+u_{nn}=u(t). \tag{A2}$$

Physically, this follows from the incompressible assumption.

The fractional flow of a phase is defined as the volume fraction of the phase flowing at a distance x and time t compared to the total flowing phase volume. For the

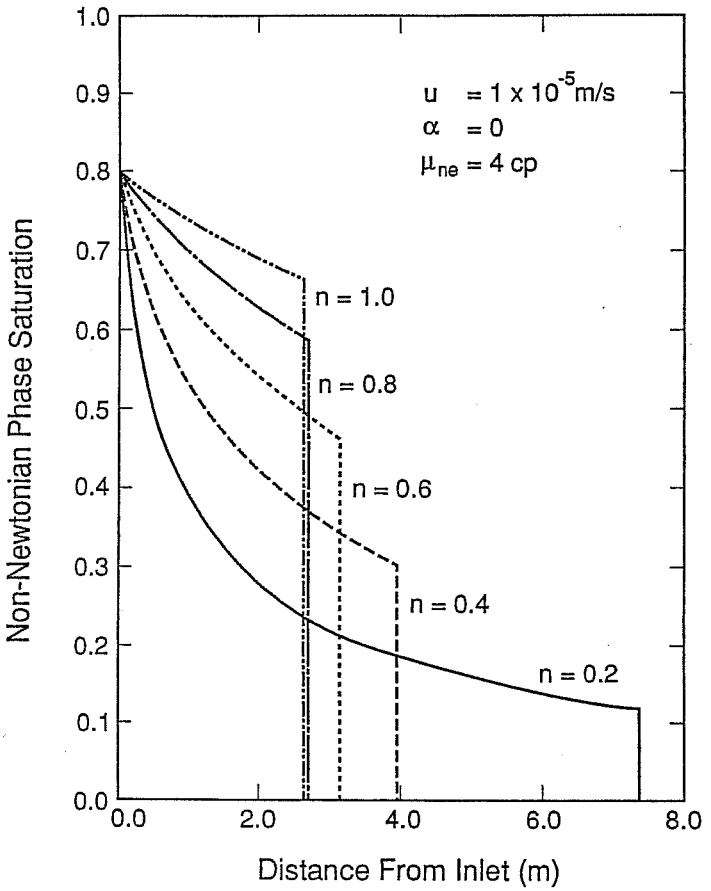

Fig. 15. Non-Newtonian phase saturation distributions; effects of the power-law index on displacement efficiency.

Newtonian phase,

$$f_{ne} = \frac{u_{ne}}{u_{ne} + u_{nn}} = \frac{u_{ne}}{u(t)} \tag{A3}$$

and, for the non-Newtonian phase,

$$f_{nn} = \frac{u_{nn}}{u_{ne} + u_{nn}} = \frac{u_{nn}}{u(t)}. \tag{A4}$$

From a volume balance, the sum of Equations (A3) and (A4) yields

$$f_{ne} + f_{nn} = 1. \tag{A5}$$

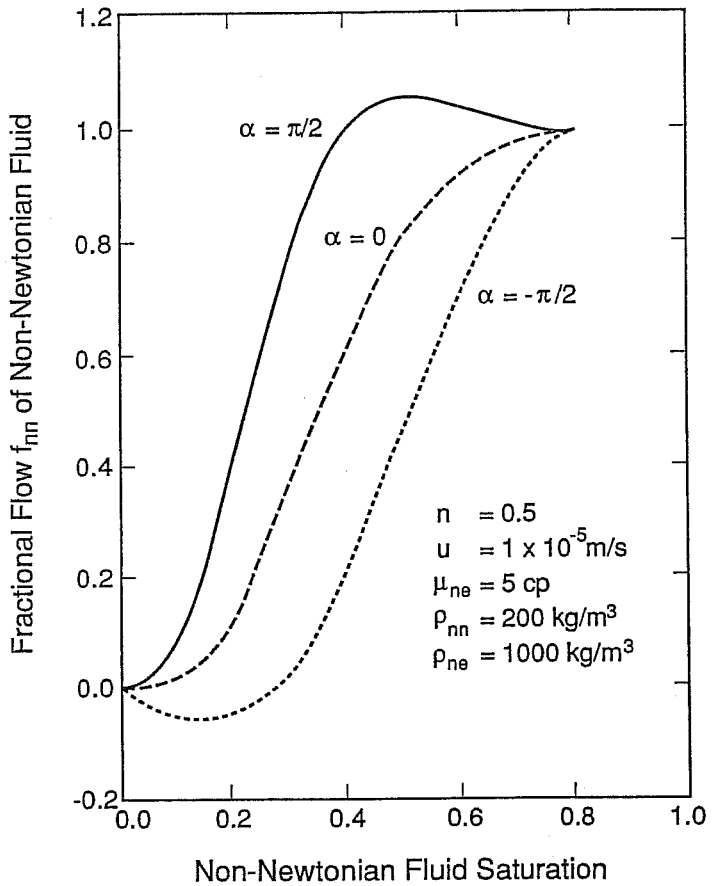

Fig. 16. Fractional flow curves including gravity effects.

Using Equations (11) and (12), Equation (A2) can be written as

$$u(t) + K\left[\frac{k_{rne}}{\mu_{ne}} + \frac{k_{rnn}}{\mu_{nn}}\right]\frac{\partial P}{\partial x} + \\ + K\left[\frac{\rho_{ne}k_{rne}}{\mu_{ne}} + \frac{\rho_{nn}k_{rnn}}{\mu_{nn}}\right]g\sin(\alpha) = 0. \tag{A6}$$

Noting that μ_{nn} is a function of both flow potential gradient and saturation from Equation (7), Equation (A6) indicates that at any given time, the potential gradient, $\partial\Phi/\partial x$, or the pressure gradient, $\partial P/\partial x$, is implicitly expressed as a function of saturation S_{nn} only (which depends on the constant angle α), or

$$\frac{\partial P}{\partial x} = \frac{\partial P}{\partial x}(S_{nn}) \tag{A7}$$

which is determined by the injection rate, relative permeability data, and non-Newtonian fluid behavior through Equation (A6).

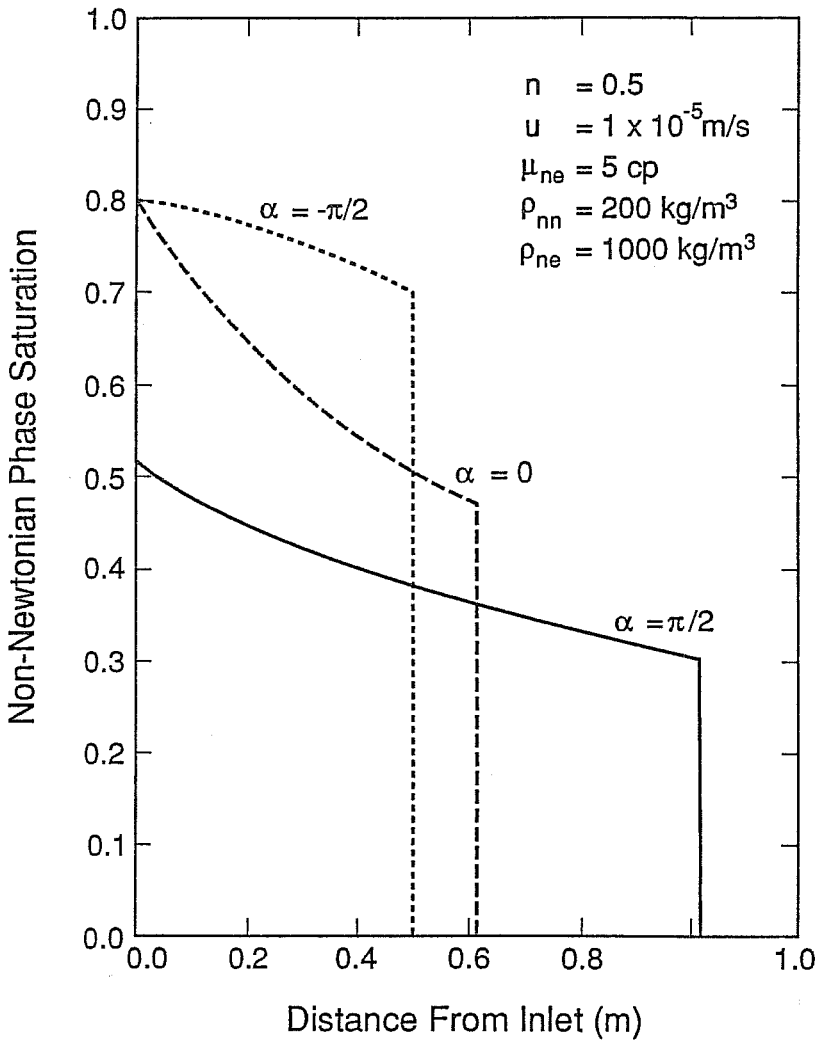

Fig. 17. Non-Newtonian phase saturation distributions; effects of gravity on displacement efficiency.

The fractional flow function for the non-Newtonian phase may be written as follows (Willhite, 1986)

$$f_{nn} = \frac{1}{1 + \left[\frac{k_{rne}}{k_{rnn}}\right]\left[\frac{\mu_{nn}}{\mu_{ne}}\right]} + \frac{\frac{Kk_{rne}}{\mu_{ne}u(t)}(\rho_{ne} - \rho_{nn})g\sin(\alpha)}{1 + \left[\frac{k_{rne}}{k_{rnn}}\right]\left[\frac{\mu_{nn}}{\mu_{ne}}\right]}, \tag{A8}$$

which is a function of S_{nn} only after considering the constraint by Equation (A6). Then, by the exact same procedure as for the Buckley and Leverett solution, we can obtain the analytical solution for non-Newtonian displacement, Equation (18).

Appendix B: Graphic Method

The mass conservation in the system for a given time of injection gives

$$Q(t) = \int_0^t q(\lambda)\, d\lambda = \int_0^{x_f} (S_{nn} - S_{nnir})\phi A\, dx$$

$$= \phi A x_f (S_f - S_{nnir}) - \int_0^{x_f} \phi A x\, dS_{nn}. \tag{B1}$$

Substituting Equation (20) into (B1) yields

$$Q(t) = Q(t)(S_f - S_{nnir}) \left[\frac{\partial f_{nn}}{\partial S_{nn}}\right]_{S_f} - Q(t)(f_{nn}|_{S_f} - f_{nn}|_0). \tag{B2}$$

Noting that at $x = 0$, $S_{nn} = 1 - S_{nnir}$, and $f_{nn} = 1$, therefore

$$1 = (S_f - S_{nnir}) \left(\frac{\partial f_{nn}}{\partial S_{nn}}\right)_{S_f} - f_{nn}|_{S_f} + 1 \tag{B3}$$

or,

$$\left(\frac{\partial f_{nn}}{\partial S_{nn}}\right)_{S_f} = \frac{f_{nn}|_{S_f} - f_{nn}|_{S_{nnir}}}{S_f - S_{nnir}} \tag{22}$$

in which $f_{nn} = 0$ at $S_{nn} = S_{nnir}$ is used, and both f_{nn} and $\partial f_{nn}/\partial S_{nn}$ are evaluated at the shock saturation S_f.

Similarly, the average saturation in the displaced zone is defined as

$$\bar{S}_{nn} = \frac{\int_0^{x_f} S_{nn} A\phi\, dx}{\int_0^{x_f} A\phi\, dx} = \frac{\phi A}{\phi A_f} \int_0^{x_f} S_{nn}\, dx \tag{B4}$$

then

$$\phi A x_f (\bar{S}_{nn} - S_{nnir}) = \phi A \int_0^{x_f} (S_{nn} - S_{nnir})\, dx = Q(t). \tag{B5}$$

Using Equation (20) again, we will have

$$\left(\frac{\partial f_{nn}}{\partial S_{nn}}\right)_{S_f} = \frac{1}{\bar{S}_{nn} - S_{nnir}}. \tag{23}$$

Appendix C: Equivalent Darcy's Law Viscosity

For a power-law non-Newtonian fluid, one describes the relationship of shear stress τ and shear rate $\dot{\gamma}$ as,

$$\tau = H\dot{\gamma}^n, \tag{C1}$$

where n and H are parameters, called power-law index and consistency of the power-law fluid. The power-law index is a dimensionless constant, and for pseudo-plastic fluids ranges over $0 < n < 1$. The consistency H has units (Pa s^n), depending on the index n. For a Newtonian fluid, $n = 1$ and the viscosity equals the constant H.

'Apparent viscosity' for a power-law non-Newtonian fluid is defined as (Ikoku and Ramey, 1980)

$$\mu_{app} = H\dot{\gamma}^{n-1}. \tag{C2}$$

For single-phase flow, the modified Blake–Kozeny equation for one-dimensional flow of power-law fluids gives (Savins, 1969; Bird *et al.*, 1960; Christopher *et al.*, 1965)

$$u = \left(\frac{K}{\mu_{eff}}\left[-\frac{\partial P}{\partial x}\right]\right)^{1/n}, \tag{C3}$$

where 'effective viscosity' μ_{eff} is defined as

$$\mu_{eff} = \frac{H}{12}\left(9 + \frac{3}{n}\right)^n (150K\phi)^{(1-n)/2}. \tag{C4}$$

For the two-phase flow problem, we extend Equation (C4) by replacing K by Kk_{mn} and ϕ by $\phi(S_{nn} - S_{nnir})$ to obtain

$$\mu_{eff} = \frac{H}{12}\left(9 + \frac{3}{n}\right)^n [150Kk_{rnn}(S_{nn})\phi(S_{nn} - S_{nnir})]^{(1-n)/2} \tag{C5}$$

In the numerical simulation, we wish to relate the volumetric flow rate to the pressure gradient as is normally done in multiple-phase extension of Darcy's law, with all of the nonlinearities combined into an equivalent non-Newtonian viscosity. Thus, we write

$$u = -\frac{Kk_{rnn}}{\mu_{nn}}\frac{\partial P}{\partial x} \tag{C6}$$

and require that this volumetric flux be equal to the expression of Equation (C3)

$$-\frac{Kk_{rnn}}{\mu_{nn}}\frac{\partial P}{dx} = \left(\frac{Kk_{rnn}}{\mu_{eff}}\left[-\frac{\partial P}{\partial x}\right]\right)^{1/n}. \tag{C7}$$

Solving for μ_{nn}, we obtain

$$\mu_{nn}\left(S_{nn}, \frac{\partial P}{\partial x}\right) = \mu_{eff}\left[\frac{Kk_{rnn}(S_{nn})}{\mu_{eff}}\left(-\frac{\partial P}{\partial x}\right)\right]^{(n-1)/n}. \tag{C8}$$

Acknowledgements

For a critical review of the manuscript and the suggestion of improvements, the authors are indebted to R. Falta and C. Radke. This work was supported, in part, by the Gas Research Institute under Contract No. 5086-271-1160, and by the Office of Basic Energy Sciences, U.S. Department of Energy, under Contract No. DE-AC03-76SF00098.

References

Bird, R. B., Stewart, W. E., and Lightfoot, E. N., 1960, *Transport Phenomena*, Wiley, New York.

Buckley, S. E. and Leverett, M. C., 1942, Mechanism of fluid displacement in sands, *Trans.* AIME **146**, 107–116.

Chen, Z. X., 1988, Some invariant solutions to two-phase fluid displacement problems including capillary effects, *SPE Reservoir Engrg.*, May, 691–700.

Christopher, R. H. and Middleman, S., 1965, Power-law flow through a packed tube, *I & EC Fundamentals* **4**, 422–426.

Fayers, F. J. and Perrine, R. L., 1959, Mathematical description of detergent flooding in oil reservoirs, *Trans.* AIME. **216**, 277–283.

Gencer, C. S. and Ikoku, C. U., 1984, Well test analysis for two-phase flow of non-Newtonian power-law and Newtonian fluids, ASME *J. Energy Resour. Technol.* June, 295–304.

Gogarty, W. B., 1967, Rheological properties of pseudo plastic fluids in porous media, *Soc. Pet. Eng. J.* June, 149–159.

Helfferich, F. G., 1981, Theory of multicomponent, multiphase displacement in porous media, *Soc. Pet. Eng. J.* Feb., 51–62.

Hirasaki, G. J., 1981, Application of the theory of multicomponent, multiphase displacement to three-component, two-phase surfactant flooding, *Soc. Pet. Eng. J.* April, 191–204.

Ikoku, C. U., 1982, Well test analysis of enhanced oil recovery project, *ASME J. Energy Resour. Technol.* June, 142–148.

Ikoku, C. U. and Ramey, H. J. Jr., 1980, Wellbore storage and skin effects during polymer flow in petroleum reservoirs, ASME. *J. Energy Resour. Technol.* Feb., 149–156.

Ikoku, C. U. and Ramey, H. J. Jr., 1979, Transient flow of non-Newtonian power-law fluids in porous media, *Soc. Pet. Eng. J.*, June, 164–174.

Larson, R. G., Davis, H. T., and Scriven, L. E., 1982, Elementary mechanism of oil recovery by chemical methods, *Soc. Pet. Eng. J.* Feb., 243–258.

Larson, R. G. and Hirasaki, G. J., 1978, Analysis of the physical mechanisms in surfactant flooding, *Soc. Pet. Eng. J.* Feb., 42–58.

Lund, O. and Ikoku, C. U., 1981, Pressure transient behavior of non-Newtonian/Newtonian fluid composite reservoirs, *Soc. Pet. Eng. J.* Apr. 271–280.

McDonald, A. E., 1979, Approximate solutions for flow of non-Newtonian power-law fluids through porous media, Paper SPE 7690 presented at the SPE-AIME Fifth Symposium on Reservoir Simulation, Denver.

Odeh, A. S. and Yang, H. T., 1979, Flow of non-Newtonian power-law fluids through porous media, *Soc. Pet. Eng. J.* June, 155–163.

Patton J. T., Coats, K. H., and Colegroue, G. T., 1971, Prediction of polymer flood performance, *Soc. Pet. Eng. J., Trans. AIME* **251**, 72–84.

Pope, G. P., 1980, The application of fractional flow theory to enhanced oil recovery, *Soc. Pet. Eng. J.*, June, 191–205.

Pruess, K., 1982, Development of the general purpose simulator MULKOM, *Annual Report*, Earth Sciences Division, Lawrence Berkeley Laboratory, Berkeley CA.

Pruess, K. and Wu, Y. -S., 1988, On PVT-data, well treatment, and preparation of input data for an isothermal gas-water-foam version of MULKOM, Report LBL-25783, UC-403, Earth Sciences Division, Lawrence Berkeley Laboratory, Berkeley, CA.

Savins, J. G., 1969, Non-Newtonian flow through porous media, *Ind. Eng. Chem.* **61**, 81–47.
Scheidegger, A. E., 1974, *The Physics of Flow Through Porous Media*, University of Toronto Press.
Sheldon, J. W., Zondek, B., and Cardwell, W. T. Jr., 1959, One-dimensional, incompressible, noncapillary, two-phase fluid flow in a porous medium, *Trans. AIME* **216**, 290–296.
Taber, J. J., Kamath, I. S. K., and Reed, R. L., 1961, Mechanism of alcohol displacement of oil from porous media, *Soc. Pet. Eng. J.* AIME. **222**, 195–209.
Van Poolen, H. K. and Jargon, J. R., 1969, Steady-state and unsteady-state flow of non-Newtonian fluids through porous media, *Soc. Pet. Eng. J. AIME*, **246**, 80–88.
Vongvuthipornchai, S. and Raghavan, R., 1987, Pressure falloff behavior in vertically fractured wells: Non-Newtonian power-law fluids, *SPE Formation Evaluation*, Dec. 573–587.
Vongvuthipornchai, S. and Raghavan, R., 1987, Well test analysis of data dominated by storage and skin: Non-Newtonian power-law fluids, *SPE Formation Evaluation* Dec., 618–628.
Wachmann, C., 1964, A mathematical theory for the displacement of oil and water by alcohol, *Soc. Pet. Eng. J.* Aug., 250–266.
Welge, H. J., 1952, A simplified method for computing oil recovery by gas or water drive, *Trans.* AIME **3**, 108.
Willhite, G. P., 1986, *Waterflooding*, SPE Textbook Series, Society of Petroleum Engineers, Richardson, TX.
Yortsos, Y. C. and Fokas, A. S., 1983, An analytical solution for linear waterflood including the effects of capillary pressure, *Soc. Pet. Eng. J.* Feb., 115–124.